NONLINEAR SOIL-STRUCTURE INTERACTION CALCULATIONS

SIMULATING THE SIMQUAKE EXPERIMENT USING STEALTH 2D

H. T. Tang
Electric Power Research Institute
Palo Alto, California 94304

R. Hofmann and G. Yee
Science Applications, Inc.
San Leandro, California 94577

D. K. Vaughan
Weidlinger Associates
Menlo Park, California 94025

SUMMARY

Transient, nonlinear soil-structure interaction (SSI) simulations of an Electric Power Research Institute (EPRI), SIMQUAKE experiment were performed using the large strain, time domain STEALTH 2D code and a cyclic, kinematically hardening cap soil model. Results from the STEALTH simulations have been compared to identical simulations performed with the TRANAL code.

INTRODUCTION

Transient, nonlinear soil-structure interaction (SSI) simulations of an Electric Power Research Institute (EPRI), SIMQUAKE experiment (ref. 1) were performed using the large strain, time domain STEALTH 2D code (ref. 2) and a cyclic, kinematically hardening cap soil model (ref. 3). Results from the STEALTH simulations have been compared to identical simulations performed with the TRANAL code (ref. 4) and will be compared to field data at a later time.

The desirability of using a large strain, nonlinear time domain approach to do certain types of SSI simulations has been established by several investigators. In particular, two studies prior to this one and also sponsored by EPRI have explored (1) the limitations of the equivalent linear method (ELM) to calculate large strain nonlinear response (ref. 5) and (2) the effect of a soil model to allow for debonding and rebonding around a rocking structure (ref. 6).

A primary emphasis in the current study was the application to SSI simulations of a mesh-interaction (slideline) algorithm developed for impact (ref. 7) and penetration events (ref. 8). The interaction algorithm is based on explicit numerical equations developed by Wilkins (ref. 9). The interaction algorithm formulation in STEALTH 2D is "strongly coupled" in that interface motion equations are centered in both time and space.

To simulate SIMQUAKE using the interaction algorithm, a modified soil island approach used by previous studies (ref. 6) was adopted. The input excitation histories around the fictitious soil island boundary were obtained by linearly interpolating the measured time-dependent ground motion data in the free field. A free-field calculation using coarse meshes in a large domain to obtain soil island input histories was therefore not required. Furthermore, the available measured data around the structure provided a validation check of the STEALTH 2D code and the interaction algorithm.

Several types of analyses were performed. One type compared calculations in which the structure was omitted and the effects of the cap versus a simple elastic model were considered. Both velocity and stress responses within the domain of the soil island were monitored. These cases provided insight into the transient wave characteristics between linear and nonlinear soil models. These calculations also provided a preliminary test of the mesh-interaction logic in which interface nodes were constrained to act as interior nodes. Another type of analysis included both the structure and the soil (cap and elastic) but did not allow debonding and rebonding. Again, velocity and stress responses surrounding the structure were compared to each other and to the previous calculations without the structure. Basic characteristics of the soil-structure interaction are revealed through such comparisons. The last class of calculations included the comparison of two debonding-rebonding logics -- one based on the mesh-interaction algorithm and the other on a constitutive tension-cutoff model.

Next are described the SIMQUAKE field tests, the soil island methodology, the STEALTH 2D code, and the slideline logic used for various aspects of the problem. Finally, the results of various calculations are presented.

DESCRIPTION OF SIMQUAKE

The purpose of the SIMQUAKE field-test series was to impose strong earthquake-like ground motions on structural models in order to evaluate (1) soil response characteristics (through laboratory and field studies) and (2) soil-structure interaction phenomenology. For the former, endochronic (ref. 10) and cap constitutive models were developed, while in the latter

category, different numerical models were used to perform pretest and post-test analyses.

The simulated earthquake test conditions were achieved by detonating two planar arrays of explosives in such a way as to yield several cycles of planar, p- and s-wave motion passing by the structures. The amplitudes and frequencies of these motions were chosen to approximate a given undamped spectrum. A plan view of the two planar arrays of explosives and five of the structural models used in the second SIMQUAKE test series is shown in figure 1a.

During the test, measurements were taken on and near the structure and in the free field. Figure 1b shows schematically the locations of the various free-field bore holes in which instruments were located. It was intended that these free field measurements would be used as "soil-island" input boundary conditions for the various calculations. The measurements taken on or near the structure were intended to be used to validate the codes and analytic methodology.

The structural models were subjected to planar test conditions. Figure 2 is a schematic of a typical axisymmetric structure. The nominal dimensions of the various structural models are listed below.

Structure Type	Diameter (ft)	Height (ft)
1.	15	22-1/2
2.	10	15
3.	5	7-1/2

One each of the type 1, 2 and 3 structural models were imbedded to 1/4 of their height in the soil using native backfill. Two type 2 structures were included -- each at a different range location. A second type 3 structure was constructed to test a seismic isolation design. A third type 3 model was free standing and filled with water to test fluid-structure interaction. The different conditions chosen intended to shed light on questions of response, scaling, backfill and depth of burial.

SOIL ISLAND METHODOLOGY

The soil island approach is a method for coupling free-field ground motions to analyses of structure-medium interaction. It allows the analyst the freedom to develop free-field ground motion in any manner which is consistent with equations of dynamic equilibrium. This includes either field

measurements or computations or both. The soil island approach has been successfully applied to a range of problems involving wave effects on protective structures.

In the first step of the soil island approach, a fictitious boundary is designated in the free field which surrounds the location of a structure; the free-field ground motions along this boundary are stored for later use. In the second step, this volume of soil referred to as the soil island is analyzed in detail using the stored free-field ground motions as boundary conditions. This reduces the structure-medium interaction model to manageable size.

The soil island concept was initially developed to analyze the response of a surface-flush military structure in a layered site subjected to outrunning ground shock from traveling airblast loading, to local airblast induced ground motion, and to the airblast itself. The outrunning response contained predominantly low frequencies because the high frequency component was filtered out by propagation over long distances through hysteretic soil. To apply the soil island method to this case, the outrunning motion was calculated with a coarse grid (adequate up to about 1 Hz) which extended about 3 miles in length and about 1 mile in depth. A fictitious soil island was defined and motions on its boundary were stored. These were subsequently applied to the boundaries of a soil island, which included the structure. The soil island consisted of sufficiently small elements to insure that the high frequency response (up to about 30 Hz), produced by the airblast and the local airblast induced ground motion, was properly represented.

A modification of the soil island approach is adopted when simulating a physical experiment such as the SIMQUAKE series of field tests. In this case the free-field calculation is eliminated and free-field velocity and acceleration gages are installed on the boundaries of the fictitious soil island. After processing, the time-phased records are used first as input to a calculation of the response of a soil island without structure. The motions in the interior of this soil island can be compared with free-field measurements at corresponding locations. The degree of favorable comparison gives valuable insight into the adequacy of the site model. Then the structural model is inserted into the soil island and the procedure is repeated to obtain soil-structure response. Due to practical limitations on the number of channels of instrumentation, there are never input time history records at all mesh points on the soil island boundaries as is required for the soil island analysis. Studies involving input from coarse mesh free-field calculations into fine mesh soil island models indicate that satisfactory input motion at a fine mesh node can be obtained by linear spatial interpolation between the two adjacent coarse mesh nodes.

Comparison between motions in the interior of the soil island and at corresponding points of the parent free-field calculation, illustrates the success of the method.

Regardless of the methods used to define free-field ground motion, the second step in the soil island approach is to designate fictitious soil islands surrounding possible structures of interest. The free-field velocity-time histories at all points on the boundary of the island are stored for future use. The boundaries of this island are chosen sufficiently far from the eventual position of the structure that, when it is included, it causes only a slight perturbation of the boundary motion. Of course the boundaries must be chosen close enough to the structure to ensure that the eventual structure-medium interaction problem is of manageable size.

The final step is to apply the free-field motions to the boundaries of a soil island including the model of the structure. Since the soil model is the same in the island and in the free field, the time phasing of the applied motion would exactly satisfy the wave equations governing motion within the island if it were not for the structure, which disturbs the free-field motions in two ways. First, there is scattering of waves which is caused by the impedance mismatch between the soil and the structure. Although the authors are unaware of prior work which would shed light on the wave lengths associated with the scattered waves, it is speculated that they are determined by the input ground motion and possibly by the characteristic length and embedment depth of the structure. The second type of disturbance arises from waves induced in the soil by motion of the structure, such as rocking and relative translation, which is commonly recognized as structure-medium interaction. The wave lengths associated with these disturbances presumably are governed by the periods of the principal modes of structure-medium interaction. In some approaches, nonreflecting boundaries are used to absorb both types of waves so that they are not reflected back to the structure and become confused with the primary structure-medium interaction. One benefit of an energy absorbing boundary is that the boundaries may be moved close to the structure with resulting savings in computer time.

In the soil island approach, the island is presumed to be sufficiently large that reflections between the boundaries and the structure are small. Reliance is placed on dispersion, geometrical attenuation and absorption of energy by material damping to reduce the error to an acceptable level.

A simple site model involving uniform properties or horizontal layering and uniform horizontal bedrock motion was adopted for this study. Though this is not necessarily a complete picture of earthquake ground

motion, it is nevertheless one which is familiar to many workers in the area of finite element simulation of structure-medium interaction. It is also simple, which helps in identifying structure-medium interaction effects.

STEALTH 2D AND SLIDELINES

STEALTH 2D is a two-dimensional, large-strain, explicit finite-difference Lagrange computer code. The most important feature of STEALTH 2D that was tested in the SIMQUAKE simulations was the multigrid slideline capability. Slideline is an historical term which identifies the logic necessary to couple two object meshes together to simulate a penetration or impact event in which relative sliding, debonding and redebonding occurs. Numerically this means that each of the interacting objects gets its interface boundary conditions from the other object. When relative motion between the objects occurs, interface boundary node locations on one object do not necessarily coincide with the locations of interface boundary nodes on the other object. In scenarios of relative sliding, the locations of interface boundary nodes are constantly changing. In cases in which debonding and rebonding occur, the interface boundary nodes are not only changing their position along their relative interface but are often spaced by regions of void.

Slidelines are also used to effect a discontinuous change in nodalization within a particular material. This capability is called "tied sliding" because nodal points are tied to the slideline, that is, no relative sliding or debonding is allowed after the original placing of the interface nodes. The nodes act as if they were interior nodes. Figure 3 shows an example of tied sliding nodes.

For the SIMQUAKE soil island geometry, there are a number of ways in which STEALTH 2D can be used to model the event. Each has distinct physical and economic advantages and disadvantages. The simplest, most rudimentary use of STEALTH 2D does not require slidelines. In this case, a rectangular domain is chosen which is bounded by the soil island boundaries on the bottom and two sides and a horizontal free surface boundary at the elevation of the top of the structure. This is shown in figure 4a. One grid is used which includes explicit air (void) regions on either side of the structure and above the ground surface. This model has one major economic disadvantage -- that of having to compute air nodes, which could just as easily be handled by using an appropriate boundary condition and by using two grids coupled through one tied slideline to define the structure. Figure 4b shows this arrangement. Neither the mesh in figure 4a nor the one in figure 4b allows for debonding and rebonding of the structure. These effects can be handled through special logic in the constitutive model for the soil zones

next to the structure. These zones can be made very small (by STEALTH mesh), and the tension-cutoff and recompression constitutive parameters can be chosen to give the effect of gap regions. One set of calculations was performed using the STEALTH mesh. A disadvantage to this approach can occur if the "gap" zones are so small that they control the time step. In SIMQUAKE, this was not the case -- the zones in the very stiff structure controlled the time step.

Another approach for modeling debonding and rebonding involves multiple grids connected by both tied and free slidelines. Several variations of this approach are shown in figures 5a and 5b. The variation shown in figure 5a was used in several SIMQUAKE simulations. Slideline #1 is tied and is used to effect a change in zoning. Slideline #2 is located at a depth coincident with the bottom of the structure. The nodalization above and below slideline #2 is identical but debonding/rebonding is allowed to occur at the base of the structure. Everywhere else the slideline is tied. A third tied slideline exists at the ground surface connecting the bottom 1/4 of the structure to the top 3/4. A potential flaw of the approach shown in figure 5a is that no kinematic debonding is allowed at the sides of the structure. If it is necessary to achieve debonding at these locations, then zone gap models would again be necessary.

To have kinematic debonding all around the structure would require the mesh shown in figure 5b. Here, slideline #1 is the same as in figure 5a, but slideline #2 is placed at the surface of the ground and around the structure as shown. This arrangement has two advantages over the previous one -- it will require slightly less computer time because there are fewer total nodes and there is no need for gap zones. The disadvantages are that the zones are not rectangles and are less accurate than their rectangular equivalents.

Two other STEALTH 2D options which can significantly reduce cost and possibly increase accuracy are available. The primary assumption required is that the structure can be treated as a rigid body. In all the meshes shown so far, the time step is controlled by zones in the structure. The sound speed in the structure is about ten times that of the soil, so that for equivalently sized zones, the global (problem) time step is 1/10th of what would be required for the soil were it to control the global time step. Assuming that the structure is at least elastic and almost rigid allows for two options to be considered -- (1) subcycling the nodalized structure at its smaller time step or (2) using a rigid body model for the structure.

One approach using the rigid body assumption for the structure is shown in figure 6. Figure 6 is a variation of figure 5b, in which the flexible structure is replaced by a rigid body model.

DESCRIPTION OF CALCULATIONS

Several SIMQUAKE calculations have been performed using three different codes -- TRANAL, FLUSH (ref. 11) and STEALTH 2D. The results presented in this paper are primarily from the STEALTH 2D calculations. However, the STEALTH results have been compared to results from TRANAL, so where necessary, TRANAL results are also presented. TRANAL and STEALTH are both explicit time domain codes. Though TRANAL is a finite-element code and STEALTH is a finite-difference code, the only major difference is that TRANAL utilizes a small strain assumption while STEALTH does not.

Table 1 summarizes the calculations presented in this paper. These include several variations of the same boundary conditions and geometry in order to determine among other things, the effect of (1) material properties and (2) debonding-rebonding logic. Two material models were used -- elastic and kinematic cap. Two debonding-rebonding logics were used -- one involved a tension-cutoff parameter in the cap material model while the other used a distinct kinematic surface.

In order to verify the STEALTH 2D tied sliding logic, three free field calculations were made. These calculations used the same soil island volume but slightly different boundary conditions from those used in subsequent SSI calculations, in which the structure was included in the mesh. Figure 7a shows the mesh used both by TRANAL and by STEALTH. Figure 7a has no slidelines. Figure 7b is the STEALTH mesh which makes use of tied sliding in order to get a greater number of zones in the region where the structure will be placed. Notice that in both cases the soil island boundary nodes are identical.

Results from these cases for the elastic material model are shown in figures 8a and 8b. These are velocity histories at the A and B locations, respectively, noted in figures 7.

The next set of calculations that were performed included the structure. The TRANAL and STEALTH meshes are shown in figures 9a and 9b. These two meshes use gapping logics in the thin zones bordering the structure. Two other STEALTH meshes were shown in figures 5a and 5b. Figure 5a displayed a grid which uses a horizontal slideline at the base of the structure. In figure 5b, a slideline separating the entire structure from the soil was used. Characteristic results from these cases are shown in figure 10. Due to page limitations for this paper, other comparisons are not shown. The results shown are typical. Detailed results will be available in the near future as an EPRI publication.

CONCLUSIONS AND SUMMARY

The results shown indicate relatively good agreement between all the STEALTH and TRANAL calculations. The differences that are seen can probably be attributed to (1) large (STEALTH) vs small (TRANAL) strain formulation and/or (2) grid discretization differences.

REFERENCES

1. C. Chan and H. T. Tang, EPRI Research Project 810 - Soil-Structure Interaction, 1976.

2. R. Hofmann, "STEALTH - A Lagrange Explicit Finite-Difference Code for Solids, Structural, and Thermohydraulic Analysis", EPRI NP-260, Vol. 1, August 1976.

3. I. S. Sandler, F. L. DiMaggio and G. Y. Baladi, "Generalized Cap Model for Geological Material", J. of Geotechnical Engineering Division, ASCE, Vol. 102, No. GT7, July 1976.

4. J. L. Baylor, J. P. Wright, C. F. Chung, "TRANAL User's Guide, Part I, (Small Strain, Small Displacement Version)", Weidlinger Assoc., Final Report Under Contract DNA 001-76-C-0125, Report No. DNA 4960F, March 1979.

5. Julio E. Valera, et al., "Study of Nonlinear Effects on One-Dimensional Earthquake Response", EPRI NP-865, August 1978.

6. J. Isenberg, D. K. Vaughan and I. Sandler, "Nonlinear Soil-Structure Interaction", EPRI NP-945, December 1978.

7. R. Hofmann, S. L. Hancock, R. L. Puthoff and M. Wohl, "Computed Response of Spherical Shielding to Impact Loading", TCAM 72-7, May 1972.

8. M. L. Wilkins, "Penetration Mechanics", UCRL-7211, November 1969.

9. M. L. Wilkins, "Calculation of Elastic-Plastic Flow", UCRL-7322-Rev. 1, January 1969.

10. H. E. Read, K. C. Valanis, "An Endochronic Constitutive Model for General Hysteretic Response of Soils", EPRI NP-957, January 1979.

11. Dilip Jhaveri, et al., "Applications in Soil-Structure Interaction", EPRI NP-1091, June 1979.

TABLE 1. - SUMMARY OF CALCULATIONS PRESENTED

Type	Code	Comments
Free Field	TRANAL	elastic
Free Field	STEALTH 2D	elastic
Free Field	STEALTH 2D	elastic, with tied slidelines
SSI	TRANAL	kinematic cyclic cap, gapping elements (Figure 9a)
SSI	STEALTH 2D	kinematic cyclic cap, gapping zones (Figure 9b)
SSI	STEALTH 2D	kinematic cyclic cap, rigid body debonding/rebonding (Figure 6)

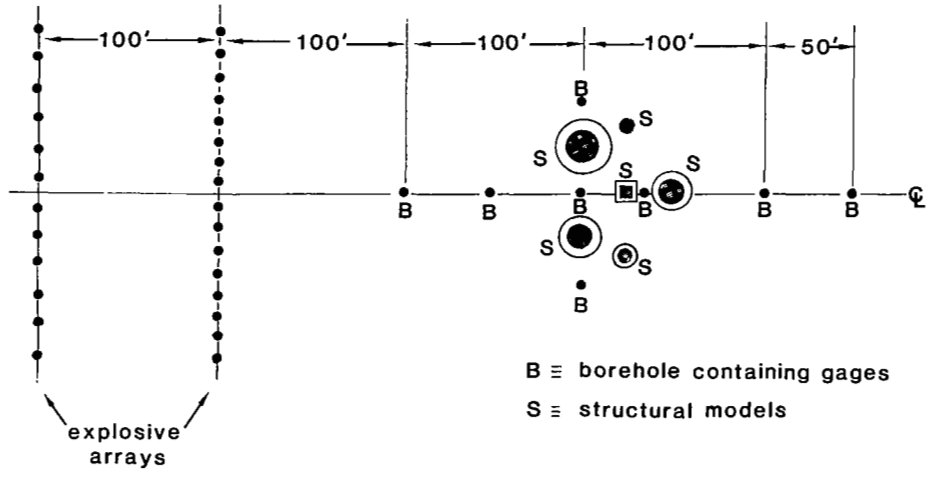

(a) Plan view.

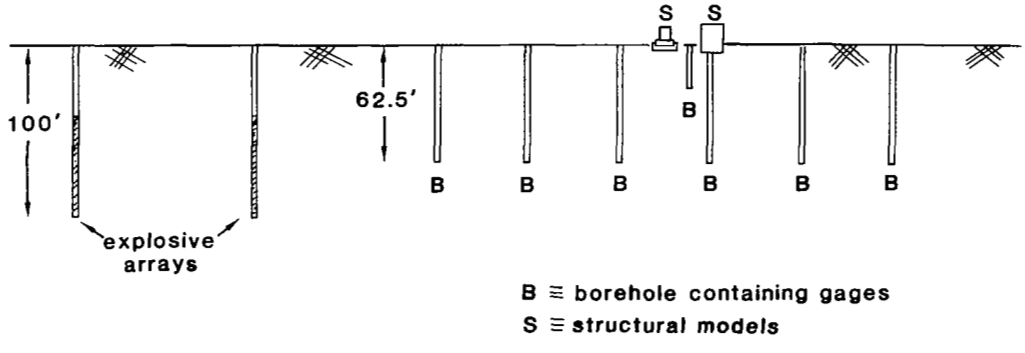

(b) Vertical cut through SIMQUAKE II centerline.

Figure 1.- SIMQUAKE II field test.

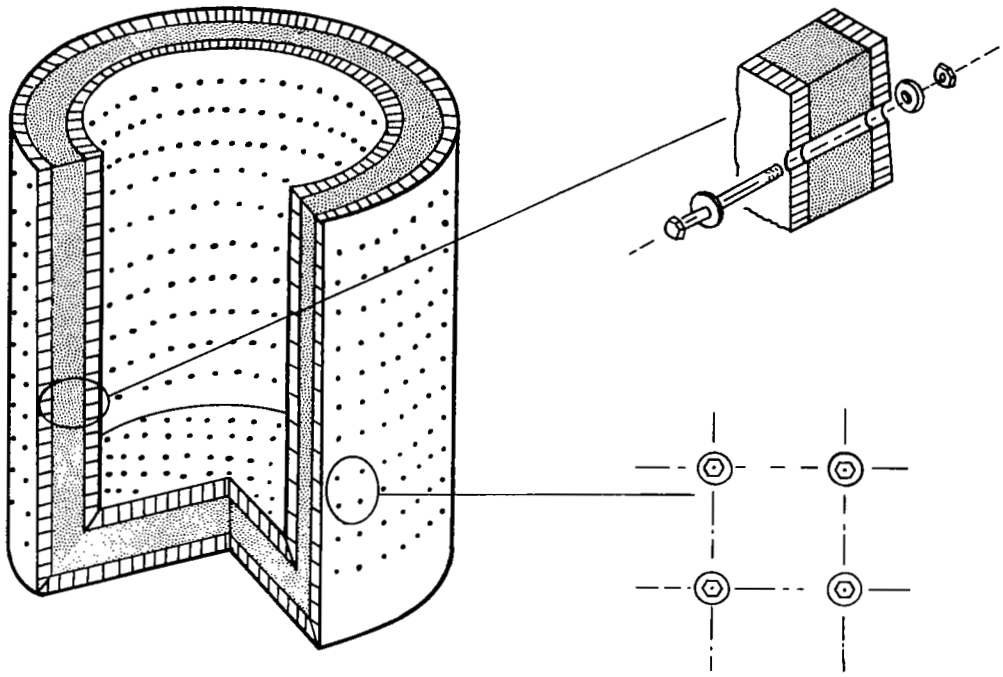

Figure 2.- Typical scaled structure.

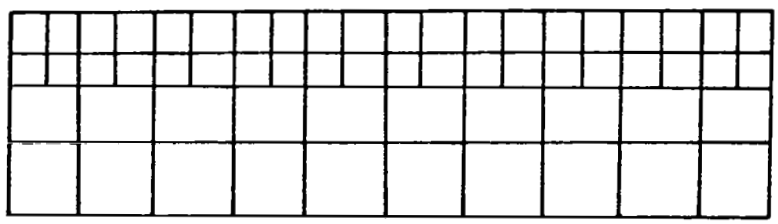

Figure 3.- Two-dimensional multi-grid example.

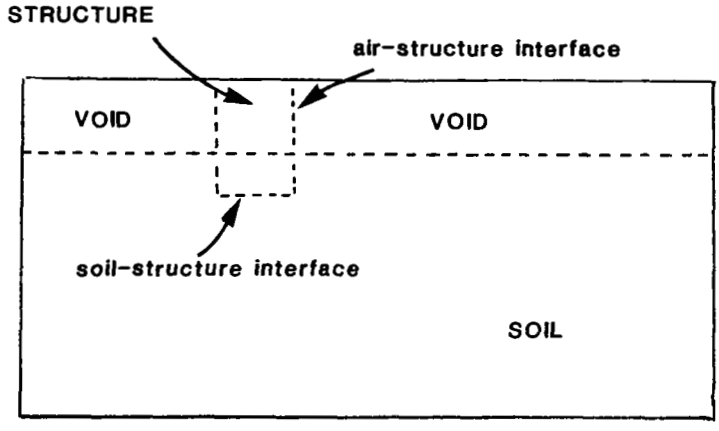

(a) Schematic using no slidelines and one grid.

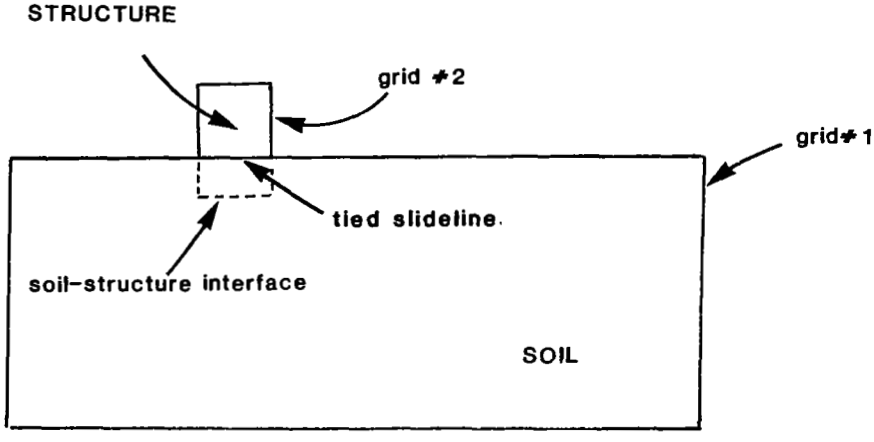

(b) Schematic using one slideline and two grids.

Figure 4.- Schematics of SIMQUAKE mesh.

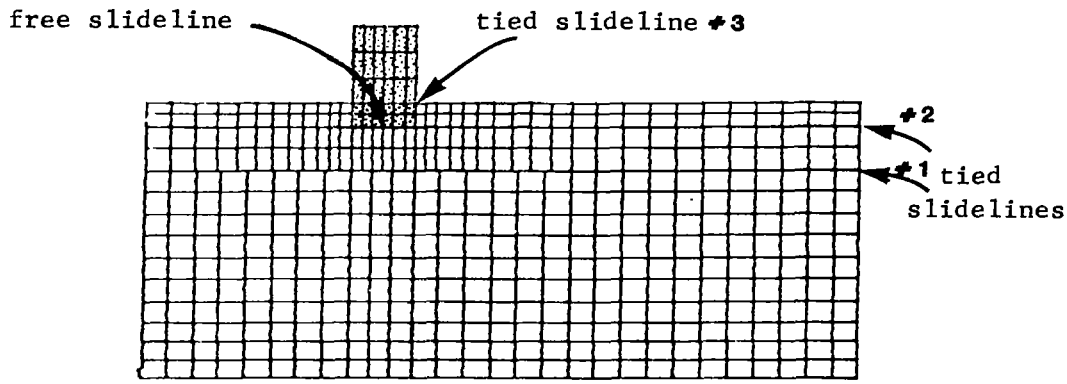

(a) At bottom of flexible structure only.

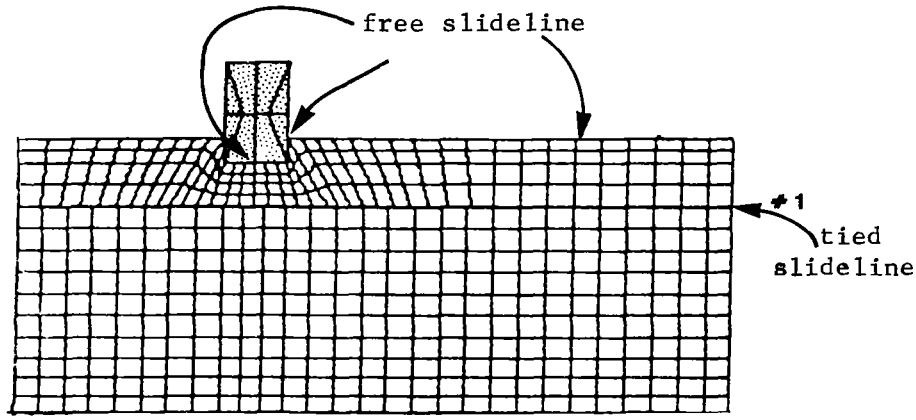

(b) All around flexible structure.

Figure 5.- Debonding/rebonding of a flexible structure.

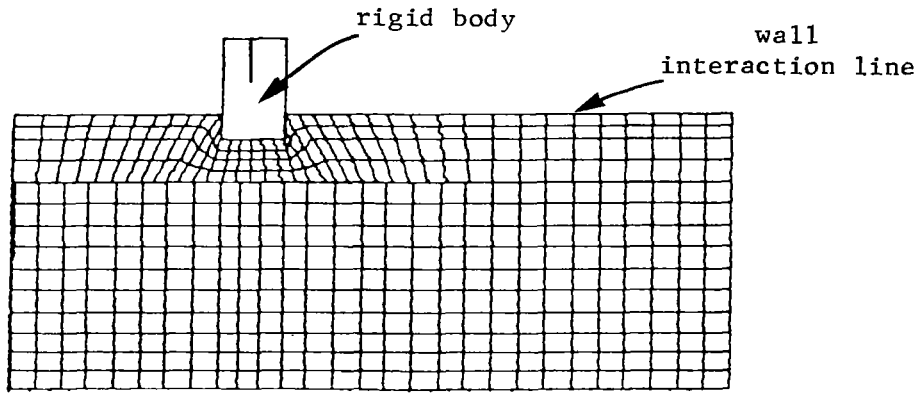

Figure 6.- Debonding/rebonding all around rigid structure.

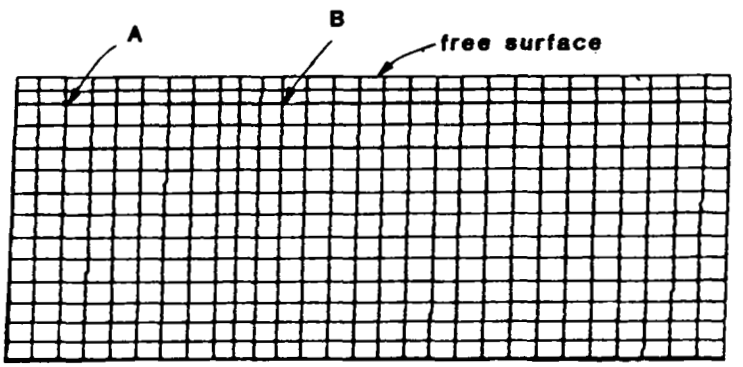

(a) TRANAL and STEALTH free field, soil island mesh using no slidelines.

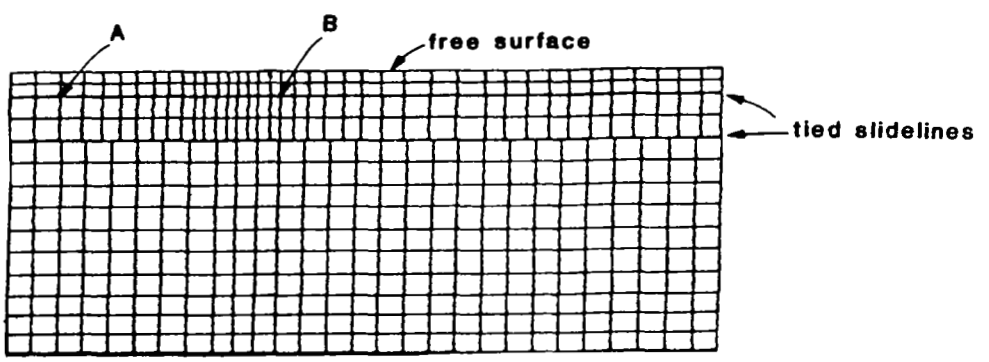

(b) STEALTH free field, soil island mesh using two tied slidelines.

Figure 7.- TRANAL and STEALTH free fields.

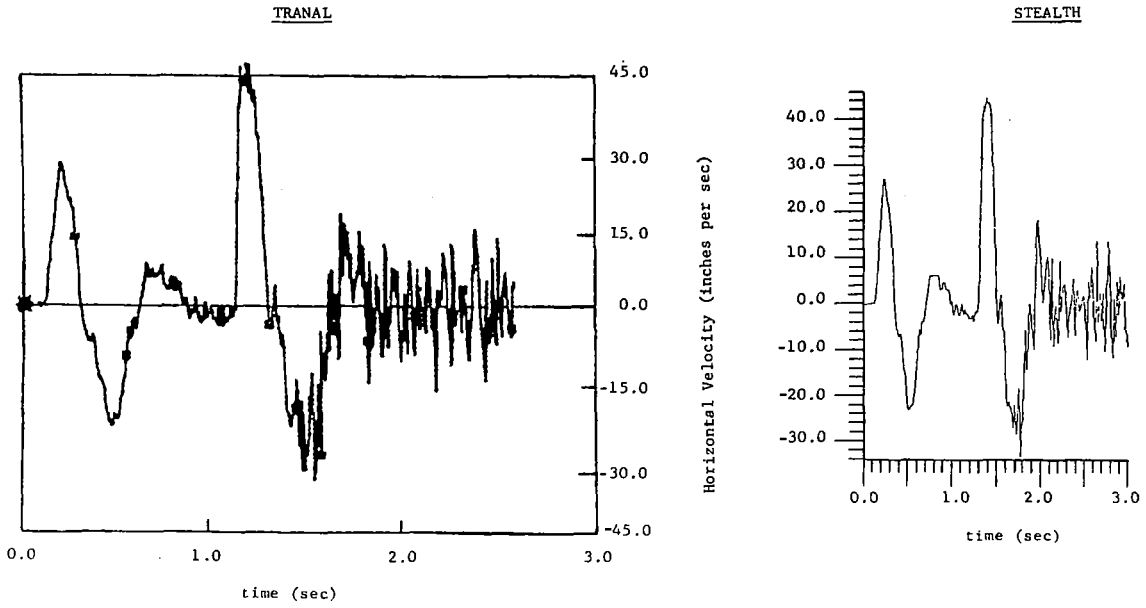

(a) Horizontal velocity histories for 3.0 seconds from TRANAL and STEALTH output at location A (see Fig. 7).

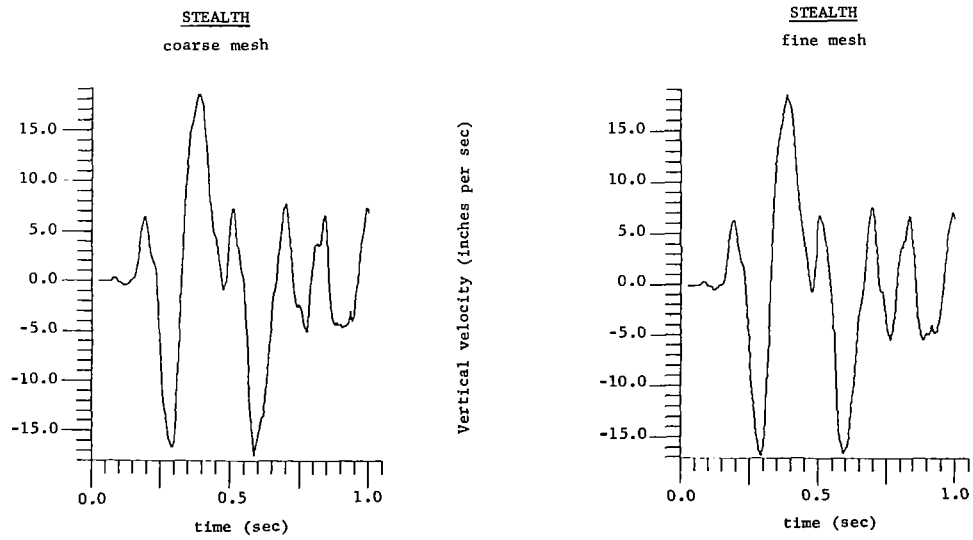

(b) Vertical velocity histories for 1.0 second from two STEALTH meshes at location B (see Fig. 7).

Figure 8.- Comparison of velocity histories for elastic free field simulations.

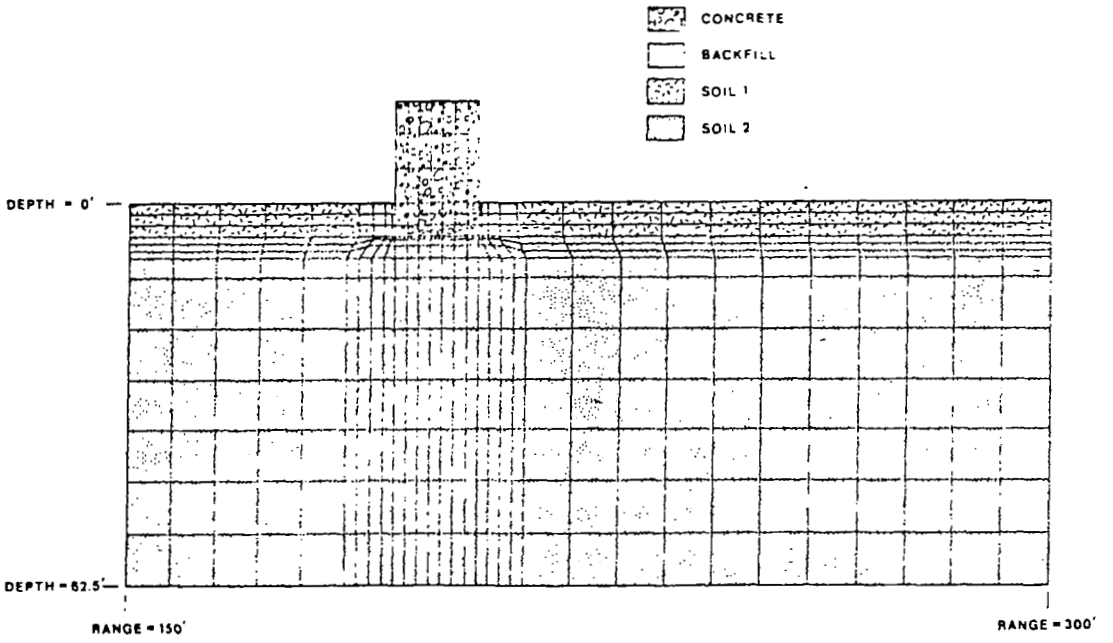

(a) TRANAL mesh.

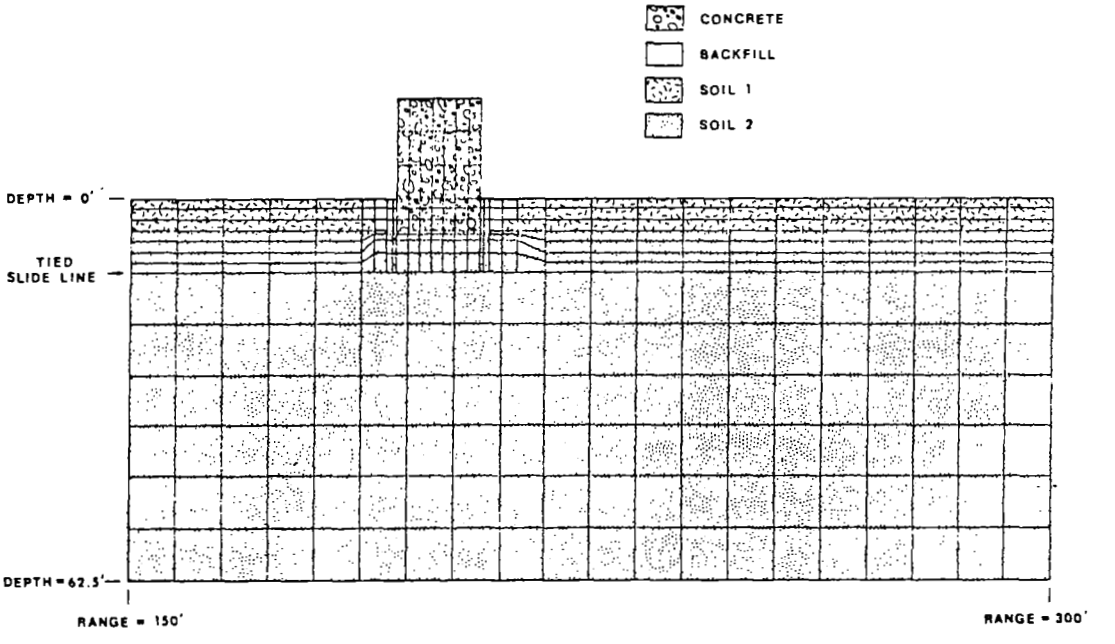

(b) STEALTH mesh.

Figure 9.- Comparison of TRANAL and STEALTH meshes with gapping elements, or zones, next to flexible structure.

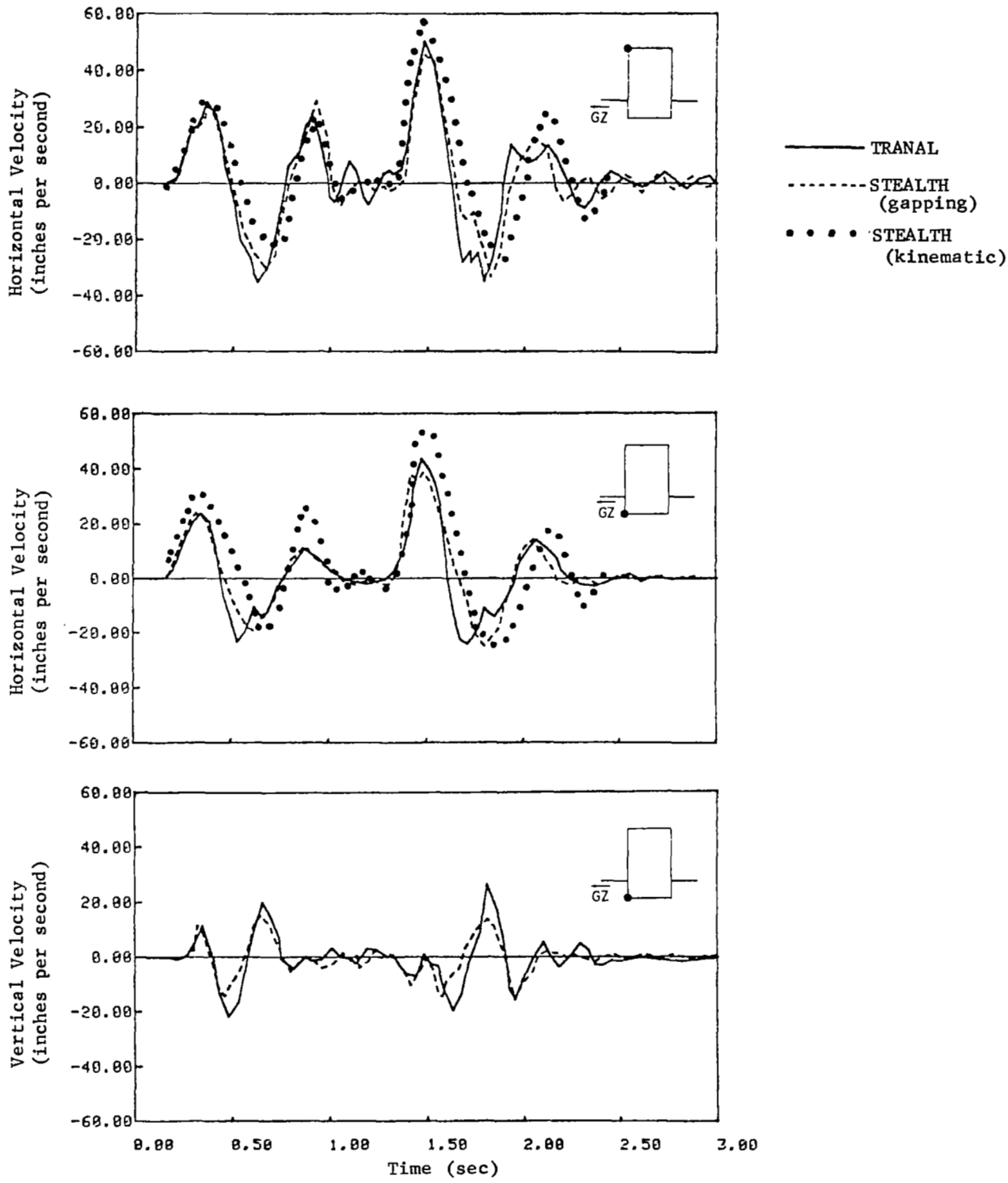

Figure 10.- Comparison of three velocity histories on the flexible structures.